Electronic Supplementary Material (ESI) for Journal of Materials Chemistry A.

Supplementary Information

Imine-based Covalent Organic Framework Gels for Efficient Removal of Fe^{2+} from contaminated water

Cristina Arqueros,[a] Lorena Welte[a], Carmen Montoro[b,c*] and Félix Zamora[b,d*]

[a.] Kleinscale, Avenida Ciudad de Valencia S/N Parque Comercial Vera Plaza, 04621, Vera-Playa, Almería, Spain.
[b.] Departamento de Química Inorgánica, Facultad de Ciencias, Universidad Autónoma de Madrid, 28049 Madrid, Spain.
[c.] Institute for Advanced Research in Chemical Sciences (IAdChem), Universidad Autónoma de Madrid, 28049 Madrid, Spain.
[d.] Condensed Matter Physics Center (IFIMAC), Universidad Autónoma de Madrid, Madrid, 28049 Spain.

Table of Contents

S1. General materials and methods

Materials. The following reagents were commercially available and were used as received:

Polysulfone (PSU, MW = 35000 g mol^{-1}), Pd/C (10 % wt), silicon tetrachloride ($SiCl_4$, 99.99 %), *N*-methyl pyrrolidone 97 % (NMP), and terephthalaldehyde (PDA, 99 %) were supplied by Sigma-Aldrich. *N,N*-dimethylformamide (DMF, HPLC grade), and tetrahydrofuran (THF) were purchased from Carlo Erba Reagents S. A.. 1,4-dioxane, mesitylene 98 %, glacial acetic acid (AcOH, 99.7 %), ethanol (EtOH, HPLC grade) and isopropyl alcohol (IPA) were acquired from Scharlab S. L.

1,3,5-tris-(4-aminophenyl) benzene (TAPB) and 2,5-dihydroxybenzene-1,4-dicarboxaldehyde (DHTA) were synthesized following reported procedures.[1, 2]

Supercritical CO_2 ($scCO_2$) activation. The solid, immersed in EtOH, was transferred into a dialysis membrane (Spectra/Por 1, MWCO: 6-8 kD) and then sealed. The membrane was introduced in the chamber of a SPI-DRY Critical Point Dryer – Jumbo, and then it was filled with liquid CO_2 and kept at 10 ºC. The membrane was immersed in CO_2(l) for 1 h to allow the exchange of solvents, and then the EtOH was removed through a purge valve followed by flushing with fresh CO_2 (l). This solvent exchange was performed in 1 h intervals until no EtOH was left in the samples. Subsequently, the temperature was raised gradually to reach 40 ºC and 90 bar to exceed the supercritical point of CO_2. Finally, under constant temperature (40 ºC), the chamber was slowly vented at 10 bar h^{-1} until atmospheric pressure was reached.

Powder X-Ray Diffraction (PXRD). PXRD patterns were collected with a Bruker D8 Advance X-ray powder diffractometer (Cu-Kα radiation; λ = 1.5418 Å) equipped with a Lynxeye detector. Samples were mounted on a flat sample plate. Patterns were collected in the 2 – 40° range with a step size of 0.03° and an exposure time of 1.3 s $step^{-1}$.

Fourier-Transform Infrared Spectroscopy (FTIR). Infrared spectra were recorded in a Perkin Elmer Spectrum 100 with a PIKE Technologies MIRacle Single Reflection Horizontal ATR accessory with a spectral range of 4000 – 400 cm^{-1}.

Solid-state ^{13}C Nuclear Magnetic Resonance (ss ^{13}C NMR) Spectroscopy. SS ^{13}C NMR spectra were recorded at room temperature on a Bruker AV 400 WB spectrometer using a triple channel, 4 mm probe with zirconia rotors, and a Kel-F cap. Cross-polarization with Magic Angle Spinning (CP-MAS) was used to acquire ^{13}C data at 100.61 MHz. Carbon chemical shifts are expressed in parts per million (δ scale) relative to tetramethylsilane as zero ppm.

Elemental Analysis (EA). EA was obtained using a LECO CHNS-932 elemental analyzer.

Scanning Electron Microscopy (SEM). SEM images were collected on a JEOL JSM 6335F scanning electron microscope at an acceleration voltage of 15 kV. Samples were dispersed over a slice of conductive adhesive adhered to a flat copper platform sample holder and then coated with 12 nm of chromium using a Quorum Q150T-S sputter coater.

Thermogravimetric Analysis (TGA). TGA samples were carried out in a thermobalance TGA Q-500 thermal gravimetric analyzer from TA Instruments. Samples were held in an aluminum pan, and N_2 was used as the purge gas. The samples were heated at 10 °C min^{-1} within a 25-1000 ZC temperature range.

N_2 adsorption-desorption isotherms. They were measured using a Micromeritics ASAP2020 volumetric instrument under static adsorption conditions. Before the measurement, samples were heated at 120 ºC overnight and outgassed to 10^{-6} Torr. Brunauer-Emmet-Teller (BET) and Langmuir analyses were carried out to determine the specific surface area values for the N_2 isotherms at 77 K. The non-local density functional theory (NLDFT) model was used to calculate the pore volume from the sorption curve using Microactive software v4.04 and considering the method based on the model N_2 at 77 K on carbon cylinder pores.

Inductively Coupled Plasma-Mass Spectrometry (ICP-MS). The concentrations were measured with an iCAP Triple quadrupole ICP-MS from Thermo Scientific. Blank standards and samples were prepared using distilled water. The samples were analyzed with a 1/10 dilution.

X-ray Photoelectron Spectroscopy (XPS). XPS analyses of COFs were performed on ground powders using a VG Escalab 200 R equipped with a hemispherical detector with 5 channeltrons (Pass energy: 2-200 eV) and a monochromatic Al Kα X-ray source (1486.61 eV). An initial survey analysis of all the samples was carried out (wide scan: step energy 1 eV, dwell time 0.1 s, pass energy 50 eV), and then a detailed analysis was performed (detail scan: step energy 0.1 eV, dwell time 0.1 s, pass energy 20 eV) with an angle of 90º for the electrons exit (normal emission).

S2. Synthesis of the materials and composites

TAPB-PDA-GCOF. It was synthesized following a previously reported procedure.[3] TAPB (500 mg, 1.42 mmol) and PDA (286 mg, 2.13 mmol) were weighed separately in 38 mL vials. TAPB was dissolved in 10 mL of AcOH and PDA in AcOH: H_2O (8 mL/2 mL). Once both monomers were completely dissolved, the aldehyde solution was rapidly added to the amine solution. A bright red gel instantly formed, and the reaction was left undisturbed for 3 days at room temperature.

TAPB-PDA-COF. The gel was washed with THF (3x100 mL), immediately turning yellow, and then with EtOH (5x100 mL). The COF was dried *via* Ar-flow drying and was activated at 120 °C under vacuum overnight, bearing a bright yellow xerogel (η = 96 %).

TAPB-DHTA-GCOF. It was synthesized following a previously reported procedure.[4] TAPB (160 mg, 0.45 mmol) and DHTA (115 mg, 0.71 mmol) were weighed in a 19 mL vial. The monomers were dissolved in a 1:4 mesitylene:*p*-dioxane solution (15 mL). Then, 10.5 M AcOH (3.4 mL) was quickly added to the monomer mixture, and a dark orange gel formed within seconds. The reaction was left undisturbed for 3 days at room temperature.

TAPB-DHTA-COF. The gel was washed with THF (3x100 mL) and EtOH (5x100 mL). The COF was dried *via sc*CO_2 drying and was activated at 120 °C under vacuum overnight, yielding a bright orange xerogel (η = 95 %).

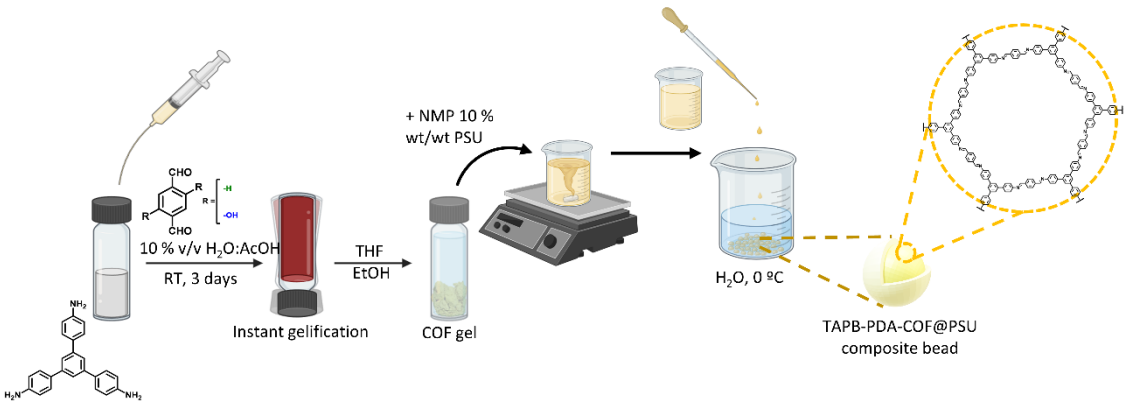

Scheme S2.1. Scheme of the preparation of TAPB-PDA-COF@PSU (b) TAPB-DHTA-COF@PSU beads.

TAPB-PDA-COF@PSU composite beads. PDA (193 mg, 1.44 mmol) and TAPB (335 mg, 0.956 mmol) were separately dissolved in 10 mL of an AcOH solution containing 10 % H_2O v/v. The PDA was rapidly added to the TAPB, and the mixture was left to react for 3 days at 35 ºC. The gel was washed with THF (3x100 mL) until the supernatant was clear. This was followed by a solvent exchange with NMP, and 5 more washes were performed. The COF was filtered with a paper filter to remove most of the solvent, so the material does not dry completely. The COF obtained was mixed with 18.80 g of the stock polymeric solution, 10 % wt. PSU in NMP. The mixture was stirred overnight at 60 ºC for complete homogenization. The polymer-COF solution was then added dropwise to a beaker filled with cold water, and the beads formed instantly in contact with water. The composite spheres were washed with distilled water to remove the NMP (5x100 mL). The solvent was exchanged with IPA (5x100 mL); the beads were dried under Ar-flow at 75 ºC after the washes. Finally, the beads were activated under vacuum at 100 ºC overnight to remove any retained solvent completely.

TAPB-DHTA-COF@PSU composite beads. DHTA (50 mg, 0.3 mmol) and TAPB (70 mg, 0.2 mmol) were dissolved in a 1:4 mesitylene:*p*-dioxane solution (10 mL). Then, 10.5 M AcOH (1.5 mL) was quickly added to the monomer mix, and the gel formed. The reaction was undisturbed for 3 days at room temperature (30 ºC). The gel was washed with THF (3x100 mL) until the supernatant was clear. They were followed by a solvent exchange with NMP (5x100 mL). The COF was filtered with a paper filter to remove the solvent, careful not to let the material completely dry. The COF was mixed with 4 g of the stock solution 10 % wt. PSU in NMP will prepare 20 % w/w COF/polymer beads. The mixture was stirred overnight at 60 ºC for complete homogenization. The polymer-COF solution was then drop-casted into a beaker filled with cold water, and the beads formed instantly. The composite spheres were washed with distilled water to remove the NMP (5x100 mL). The solvent was exchanged with IPA (5x100 mL); after the washes were performed, the beads were dried under Ar-flow at 75 ºC. Finally, the beads were activated under vacuum at 100 ºC overnight to ensure the removal of any remaining solvent.

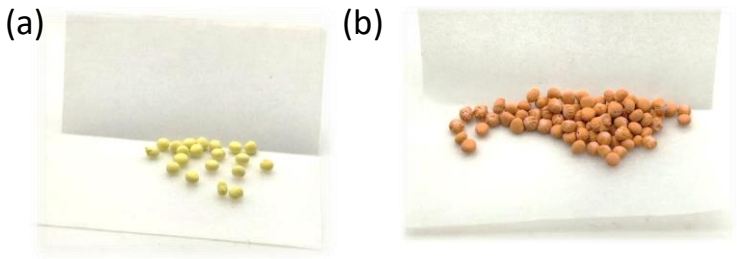

Figure S2.1. (a) TAPB-PDA-COF@PSU beads and (b) TAPB-DHTA-COF@PSU beads.

S3. Powder X-Ray Diffraction (PXRD)

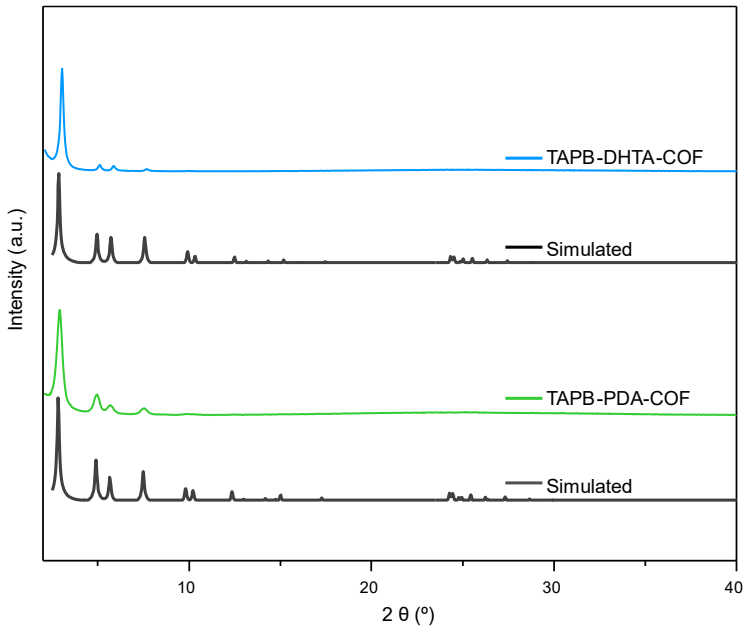

Figure S3.1 PXRD patterns of **TAPB-PDA-COF** and **TAPB-DHTA-COF** and their simulated ones.

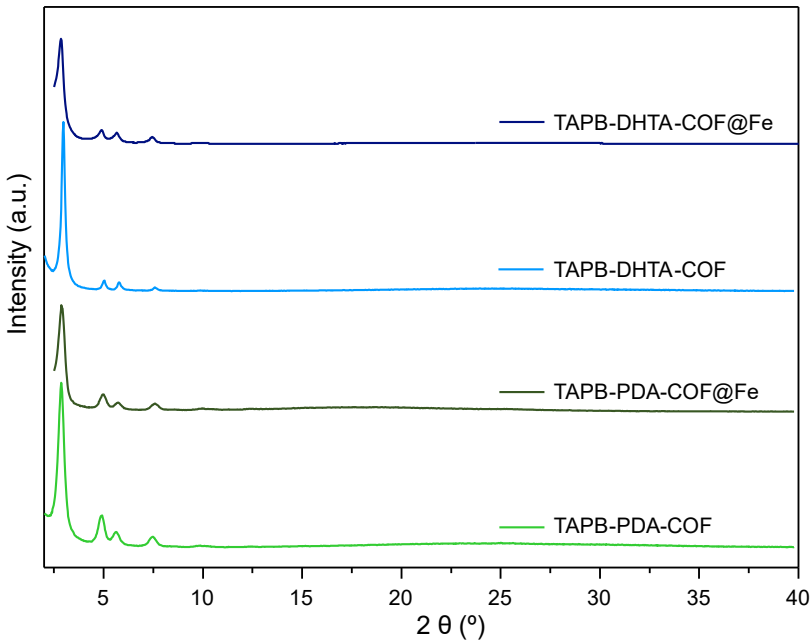

Figure S3.2. PXRD patterns before and after the capture studies of Fe^{2+} in waters. **TAPB-PDA-COF** and **TAPB-DHTA-COF** before and after.

S4. Fourier-Transform Infrared Spectroscopy (FTIR)

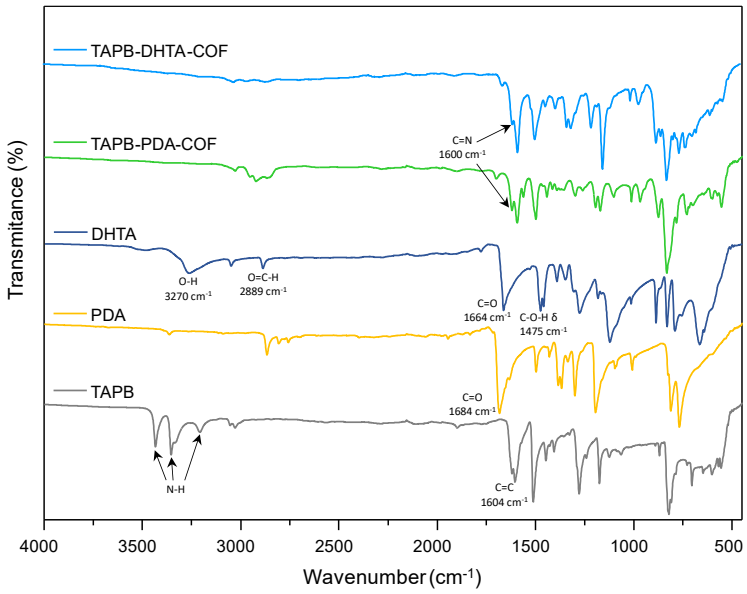

Figure S4.1. FTIR spectra of **TAPB-PDA-COF**, **TAPB-DHTA-COF**, TAPB, DHTA, and PDA.

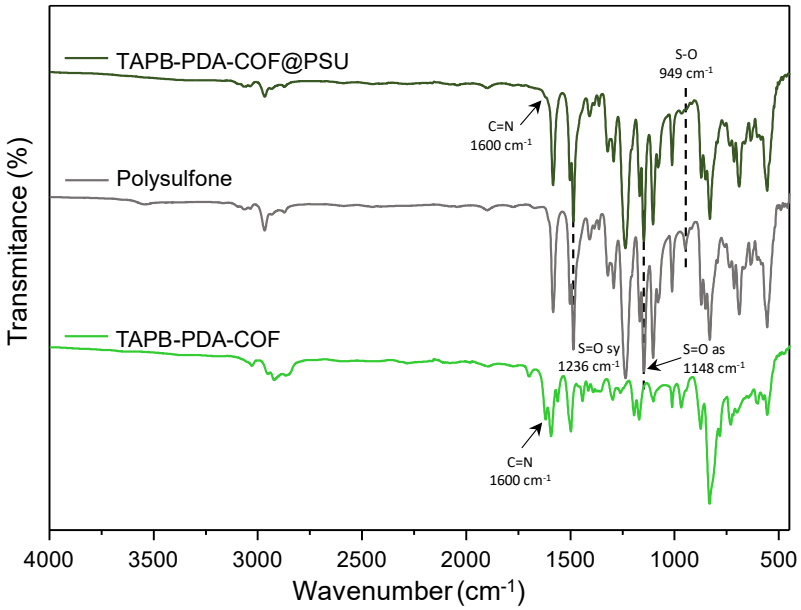

Figure S4.2. FTIR spectra of **TAPB-PDA-COF@PSU** composite beads, PSU, and **TAPB-PDA-COF**.

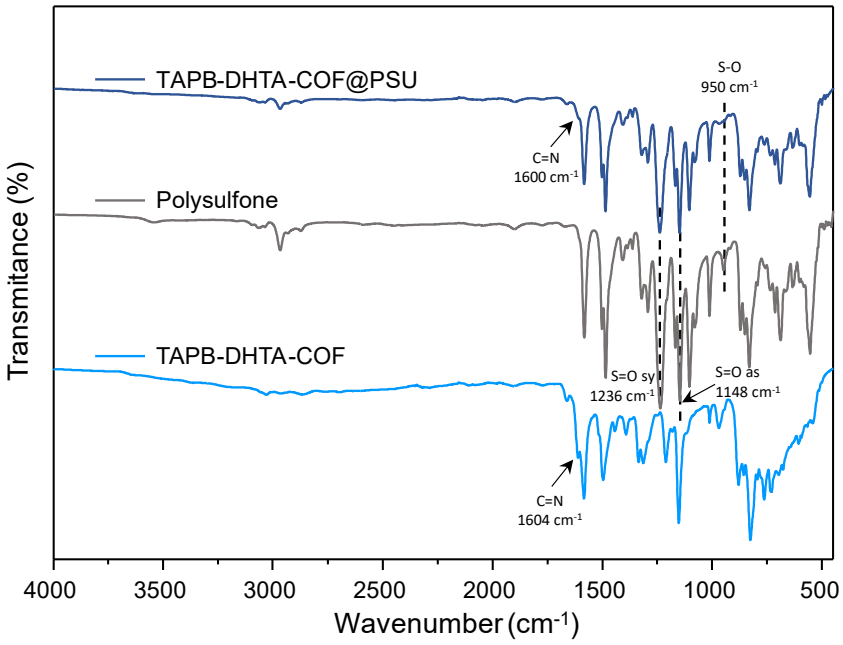

Figure S4.3. FTIR spectra of **TAPB-DHTA-COF@PSU** composite beads, PSU, and **TAPB-PDA-COF**.

S5. Solid-State ^{13}C Nuclear Magnetic Resonance (ss ^{13}C NMR) Spectroscopy

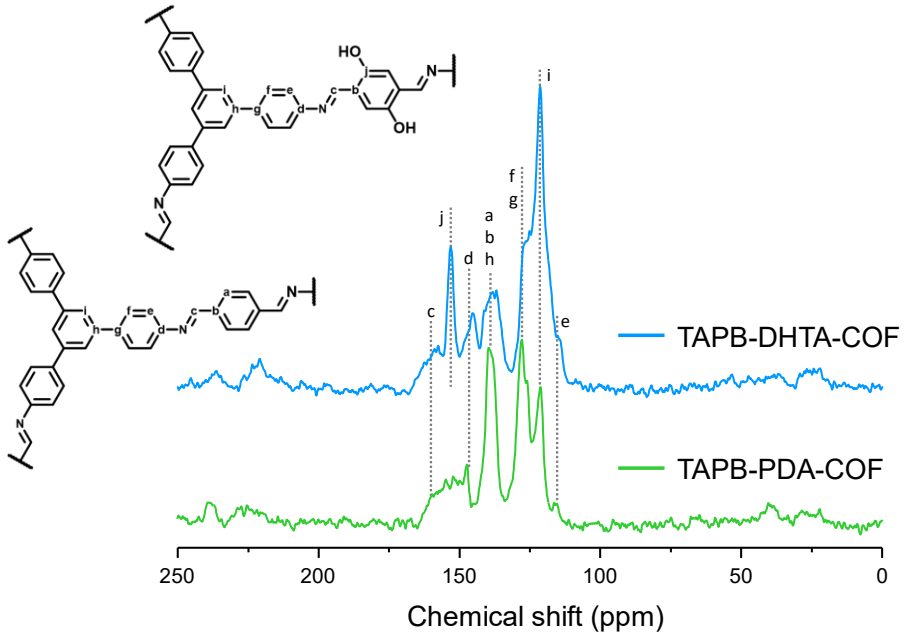

Figure S5.1. ss ^{13}C CP-MAS NMR spectra of **TAPB-PDA-COF** and **TAPB-DHTA-COF**.

S6. Elemental Analysis (EA)

Table S6.1. Composition of **TAPB-PDA-COF** and **TAPB-DHTA-COF** obtained by EA.

Material	Molecular weight (g mol^{-1})	Formula	% C	% H	% N
TAPB-PDA-COF	997.0	$C_{72}H_{48}N_6$	84.65	5.34	8.06
TAPB-DHTA-COF	1092.0	$C_{72}H_{48}N_6O_6$	77.10	4.92	7.45

S7. Scanning Electron Microscopy (SEM)

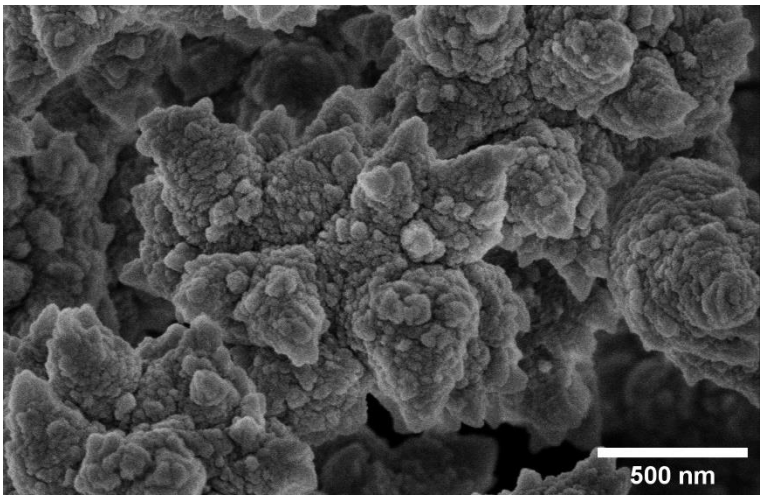

Figure S7.1 SEM images of **TAPB-DTHA-COF** after the removal studies.

S8. Thermogravimetric Analysis (TGA)

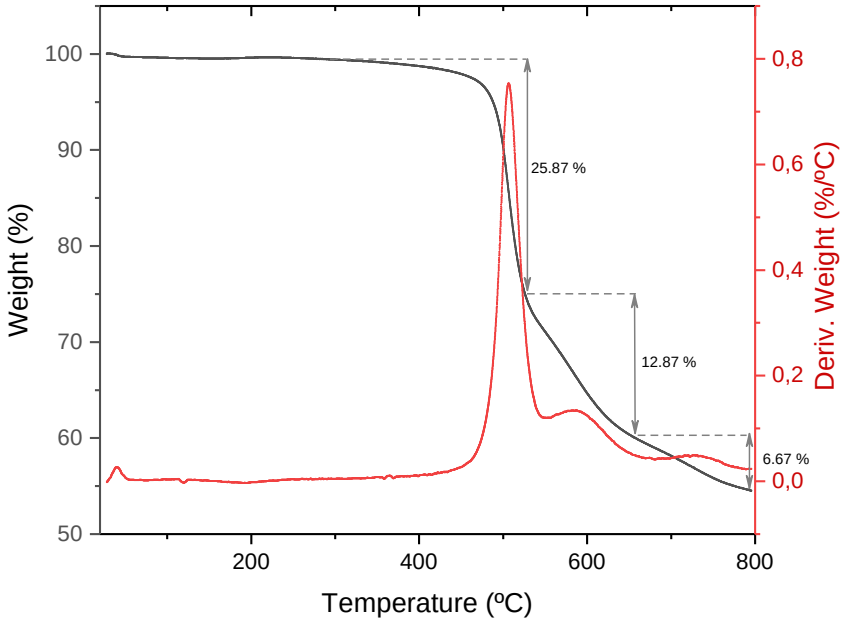

Figure S8.1. TGA profile of **TAPB-PDA-COF.**

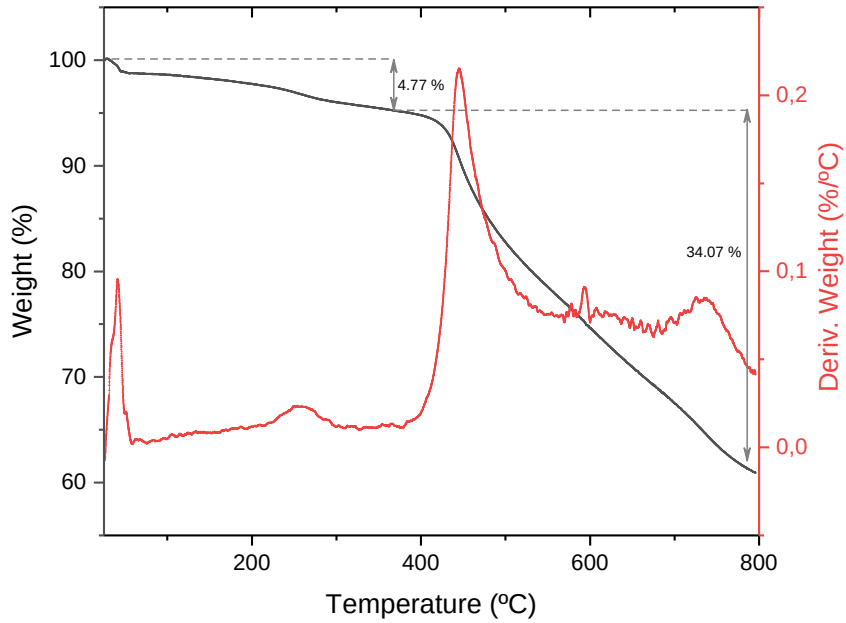

Figure S8.2. TGA profile of **TAPB-DHTA-COF.**

S9. Nitrogen adsorption and desorption isotherms

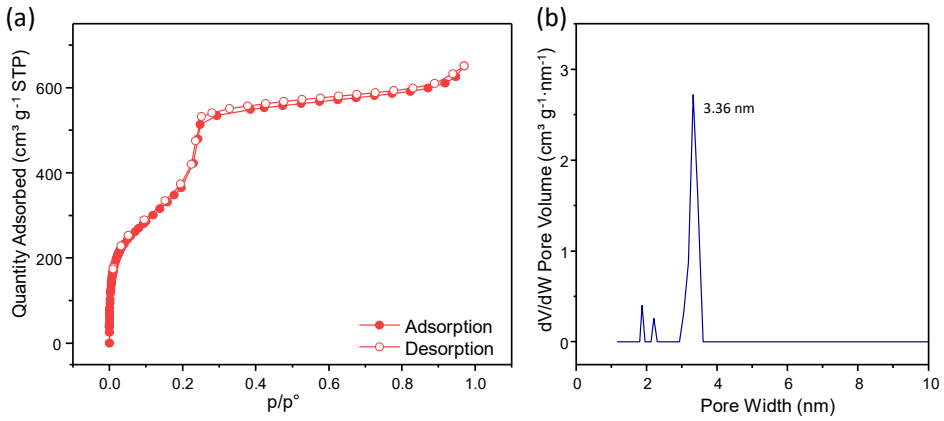

Figure S9.1. (a) N_2 adsorption-desorption isotherms and (b) pore size of **TAPB-PDA-COF**.

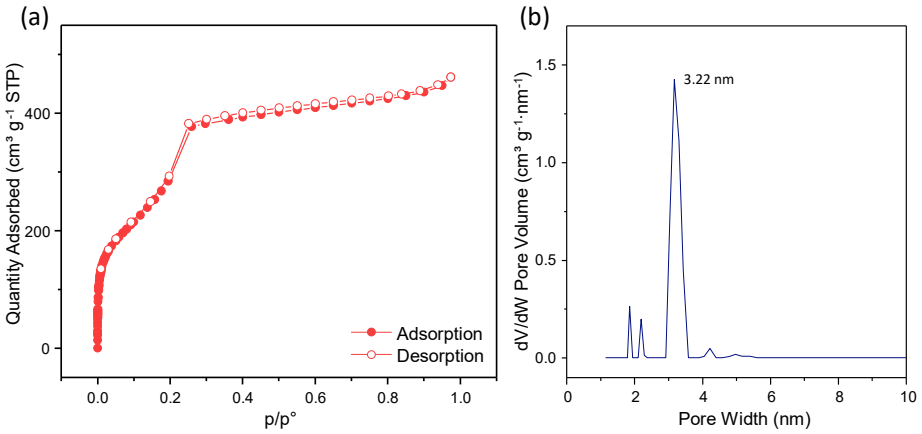

Figure S9.2. (a) N_2 adsorption-desorption isotherms and (b) pore size of **TAPB-DHTA-COF**.

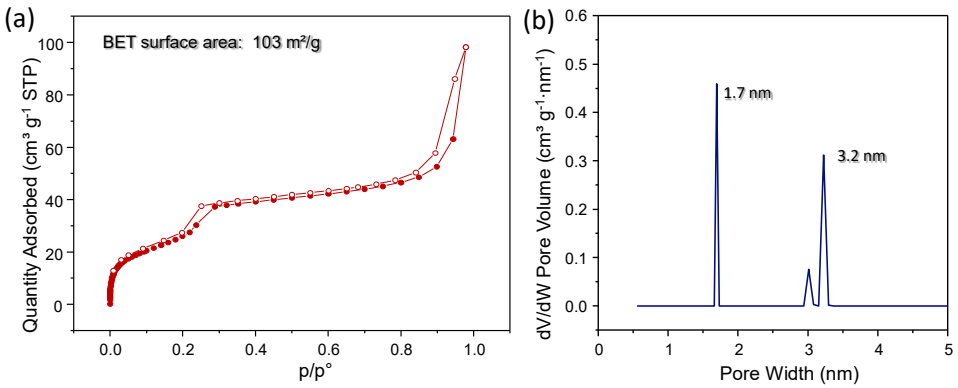

Figure S9.3. (a) N_2 adsorption-desorption isotherm and (b) pore size for **TAPB-PDA-COF@PSU** composite beads.

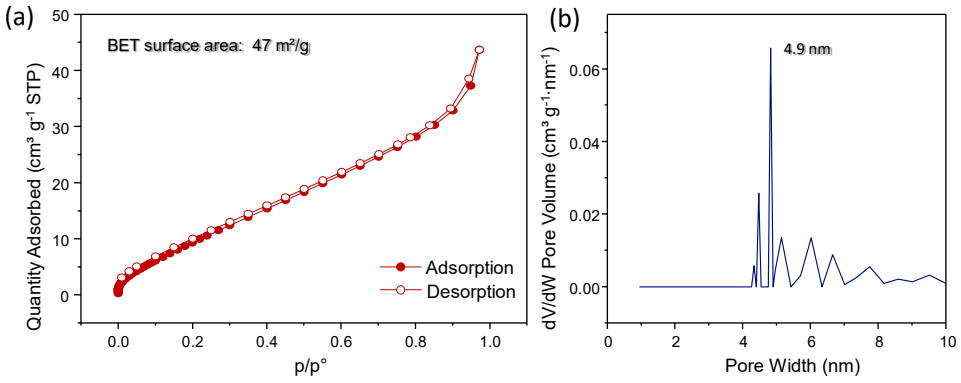

Figure S9.4. (a) N_2 adsorption-desorption isotherm and (b) pore size for **TAPB-DHTA-COF@PSU** composite beads.

S10. Additional data from the adsorption studies

Table S10.1. Data from the pH dependence study of **TAPB-PDA-COF** in the removal of Fe^{2+} ions from water. Experimental conditions: T = 298 K, time = 1 h, V = 15 mL, salt: $FeCl_2{\cdot}4H_2O$.

m (mg)	pH	C_i (mg L^{-1})	C_f (mg L^{-1})	% Retention	Q_e (mg g^{-1})
10.0	3.50	1.01	0.59	42	0.629
10.3	5.50	1.00	0.22	78	1.140
10.4	8.32	0.89	0.00	100	1.286
10.1	10.11	0.97	0.36	63	0.905
10.0	11.50	1.03	0.87	16	0.240

Table S10.2. Data from the pH dependence study of **TAPB-DHTA-COF** in the removal of Fe^{2+} ions from water. Experimental conditions: T = 298 K, time = 1 h, V = 15 mL, salt: $FeCl_2{\cdot}4H_2O$.

m (mg)	pH	C_i (mg L^{-1})	C_f (mg L^{-1})	% Retention	Q_e (mg g^{-1})
10.2	3.50	1.01	0.55	46	0.678
10.1	5.50	1.00	0.19	81	1.209
10.5	8.32	0.89	0.01	99	1.255
10.3	10.11	0.97	0.31	68	0.966
10.2	11.50	1.03	0.38	63	0.959

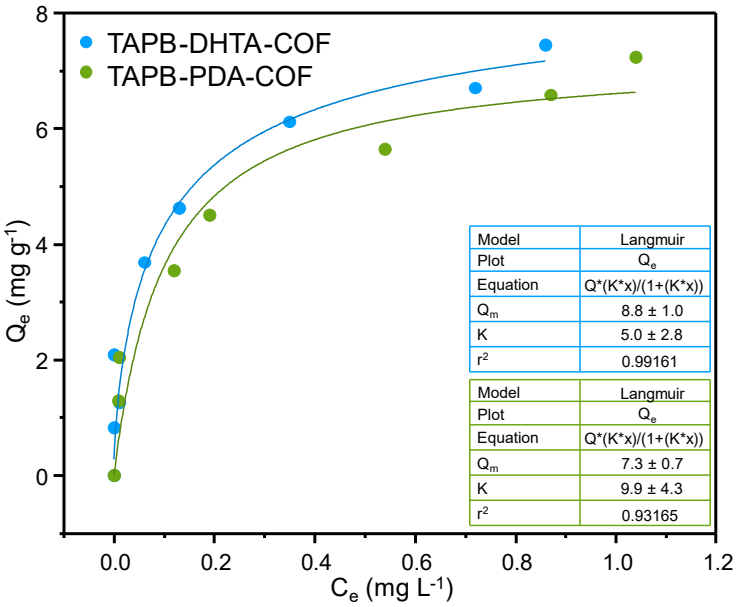

Figure S10.1. Adsorption isotherms of **TAPB-PDA-COF** and **TAPB-DTHA-COF**. Inset: Fitting Langmuir isotherm model.

Table S10.3. Data from the adsorption isotherm of **TAPB-PDA-COF** towards Fe^{2+}. Experimental conditions: T = 298 K, time = 1 h, V = 25 mL, salt: $FeCl_2 \cdot 4H_2O$.

m (mg)	C_i (mg L^{-1})	C_f (mg L^{-1})	% Retention	Q_e (mg g^{-1})
10.0	0	0	0	0
10.4	0.890	0.009	99	1.273
10.2	0.840	0.010	99	2.040
10.1	1.550	0.120	92	3.543
10.5	2.090	0.190	91	4.502
10.0	2.790	0.540	81	5.636
9.9	3.490	0.870	75	6.583
10.1	3.960	1.040	74	7.235

Table S10.4. Data from the adsorption isotherm of **TAPB-DHTA-COF** towards Fe^{2+}. Experimental conditions: T = 298 K, time = 1 h, V = 25 mL, salt: $FeCl_2 \cdot 4H_2O$.

m (mg)	C_i (mg L^{-1})	C_f (mg L^{-1})	% Retention	Q_e (mg g^{-1})
10.09	0	0	0	0
10.07	0.33	0.00	100	0.818
10.52	0.84	0.00	100	2.085
10.11	0.89	0.01	99	1.255
10.60	1.55	0.06	96	3.684
9.98	2.09	0.13	94	4.623
10.33	2.79	0.35	87	6.112
10.40	3.49	0.72	79	6.704
10.09	3.96	0.86	78	7.452

Table S10.5. Data from the adsorption kinetic of **TAPB-PDA-COF** towards Fe^{2+}. Experimental conditions: T = 298 K, c = 1 ppm, salt: $FeCl_2 \cdot 4H_2O$. The experiment was carried out three times and C_{f1}, C_{f2} and C_{f3} correspond to the final concentration measured each time.

m (mg)	t (min)	C_i (mg L^{-1})	C_{f1} (mg L^{-1})	C_{f2} (mg L^{-1})	C_{f3} (mg L^{-1})	% Retention	Q_t (mg g^{-1})
0	0	0.97	0.000	0.000	0.000	0	0.0000
9.5	5	0.97	0.14	0.14	0.15	85	1.3053
9.4	10	0.97	0.16	0.16	0.17	83	1.2872
9.6	15	0.97	0.14	0.14	0.15	85	1.2917
9.8	30	0.97	0.17	0.17	0.19	82	1.2143
9.5	60	0.97	0.17	0.17	0.19	82	1.2526
10.2	240	0.97	0.090	0.09	0.09	91	1.2941

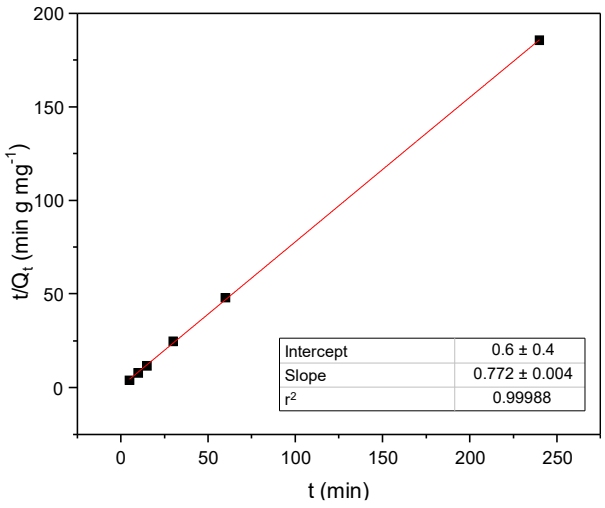

Figure S10.2. TAPB-PDA-COF adsorption kinetics linear fitting, t/Q_t vs *time*.

Table S10.6. Data from the adsorption kinetic of **TAPB-DHTA-COF** towards Fe^{2+}. Experimental conditions: T = 298 K, c = 1 ppm, salt: $FeCl_2 \cdot 4H_2O$. The experiment was carried out three times and C_{f1}, C_{f2} and C_{f3} correspond to the final concentration measured each time.

m (mg)	t (min)	C_i (mg L^{-1})	C_{f1} (mg L^{-1})	C_{f2} (mg L^{-1})	C_{f3} (mg L^{-1})	% Retention	Q_t (mg g^{-1})
0	0	0.97	0.000			0	0.0000
9.2	5	0.97	0.23	0.24	0.25	75	1.1902
10.2	10	0.97	0.25	0.23	0.25	75	1.0686
9.4	20	0.97	0.25	0.24	0.26	74	1.1489
9.6	30	0.97	0.20	0.20	0.20	79	1.2031
9.6	60	0.97	0.17	0.17	0.17	82	1.2500
9.5	240	0.97	0.13	0.13	0.13	87	1.3263

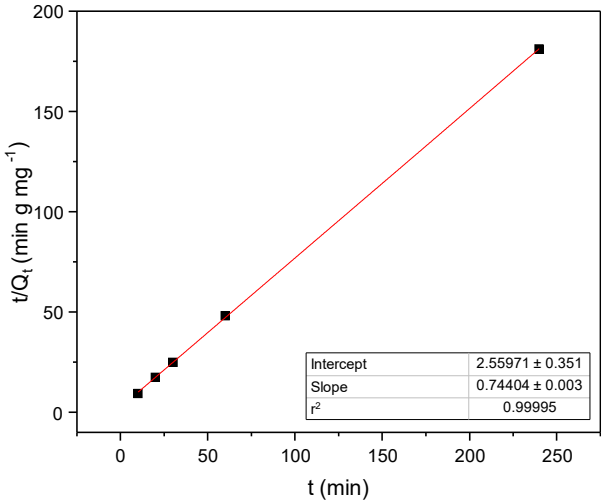

Figure S10.3. TAPB-DHTA-COF adsorption kinetics linear fitting, t/Q_t vs *time*.

Table S10.7. Adsorption capacities of different reported adsorbents for the removal of Fe^2 from water.

Material	$Q_{máx}$ (mg g^{-1})	pH	Ref.
TAPB-PDA-COF	7.3	6-7	This work
TAPB-DHTA-COF	8.8	6-7	This work
Iron oxide-coated hollow polymethylmethacrylate microspheres	2.6	7	[5]
Bentonite clay	64.94	3	[6]
Magnetic Graphene Oxide (MGO)	43.2	5.5	[7]
Granular activated carbon	3.6	-	[8]
AC derived from agro-residues	0.8	-	[9]
Natural zeolite	1.1	7	[10]
Adsorbent coal	15	7	[11]
COF@PDA	204.9	6	[12]

S11. X-ray Photoelectron Spectroscopy (XPS)

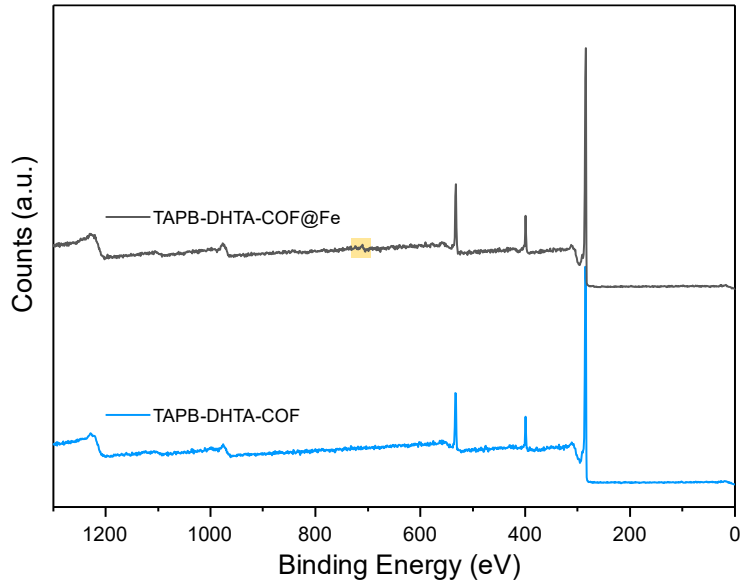

Figure S11.1. Comparative XPS spectra of the pristine **TAPB-DHTA-COF** and **TAPB-DHTA-COF@Fe**.

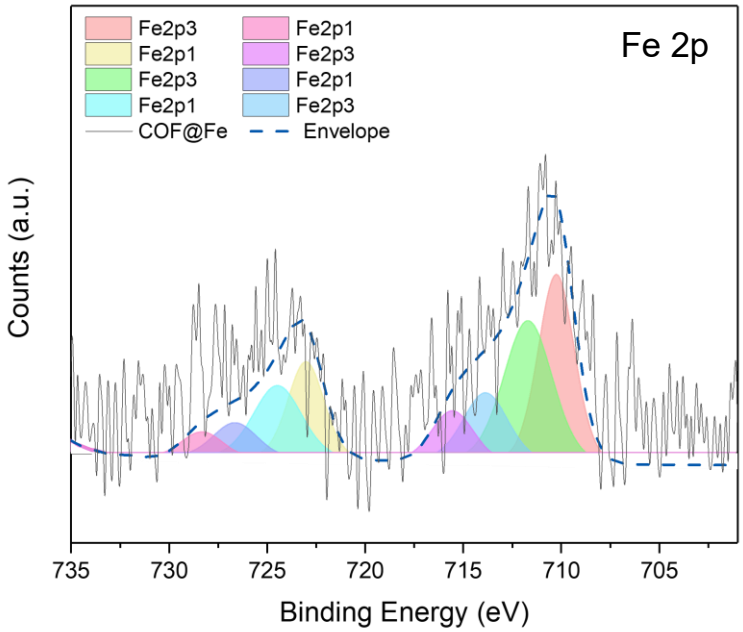

Figure S11.2. XPS data for Fe 2p core level spectrum of **TAPB-DHTA-COF@Fe,** including a line shape analysis and deconvolution of the peaks.

S12. References

1 A. de la Peña Ruigómez, D. Rodríguez-San-Miguel, K. C. Stylianou, M. Cavallini, D. Gentili, F. Liscio, S. Milita, O. M. Roscioni, M. L. Ruiz-González, C. Carbonell, D. Maspoch, R. Mas-Ballesté, J. L. Segura and F. Zamora, *Chemistry Eur. J.*, 2015, **21**, 10666–10670.

2 H. Xu, J. Gao and D. Jiang, *Nat. Chem.*, 2015, **7**, 905–912.

3 J. Á. Martín-Illán, D. Rodríguez-San-Miguel, O. Castillo, G. Beobide, J. Perez-Carvajal, I. Imaz, D. Maspoch and F. Zamora, *Angew. Chem. Int. Ed.*, 2021, **60**, 13969–13977.

4 C. H. Feriante, S. Jhulki, A. M. Evans, R. R. Dasari, K. Slicker, W. R. Dichtel and S. R. Marder, *Adv. Mater.*, 2020, **32**, 1905776.

5 D. Dutta, R. Dubey, S. Banerjee, J. P. Borah and A. Puzari, *Environ. Chall.*, 2021, **4**, 100115.

6 S. S. Tahir and N. Rauf, *J. Environ. Manage.*, 2004, **73**, 285–292.

7 H. Yan, H. Li, X. Tao, K. Li, H. Yang, A. Li, S. Xiao and R. Cheng, *ACS Appl. Mater. Interf.*, 2014, **6**, 9871–9880.

8 A. bin Jusoh, W. H. Cheng, W. M. Low, A. Nora'aini and M. J. Megat Mohd Noor, *Desalination*, 2005, **182**, 347–353.

9 Magda A. Akl*, AbdElFatah M. Yousef and Sameh AbdElnasser, *J. Chem. Eng. Process. Tech.*, 2013, **4**, 1–10.

10 M. A. Shavandi, Z. Haddadian, M. H. S. Ismail, N. Abdullah and Z. Z. Abidin, *J. Taiwan Inst. Chem. Eng.*, 2012, **43**, 750–759.

11 J. P. Vistuba, M. E. Nagel-Hassemer, F. R. Lapolli and M. Á. Lobo Recio, *Environ. Technol.*, 2013, **34**, 275–282.

12 Y. Xiao, C. Ma, Z. Jin, J. Wang, L. He, X. Mu, L. Song and Y. Hu, *Chem.l Eng. J.*, 2021, **421**, 127837.